Al-Kufa University Journal for Biology / VOL.14 / NO.3 / Year: 2022
Print ISSN: 2073-8854 Online ISSN: 2311-6544

Ameliorative and protective activity of Silver Nanoparticles (AgNPs) Biosynthesized Using *Taraxacum officinale* L. leaves Extract against 1, 2-dimethylhydrazine (DMH) Induced Colon Cancer in Rats

Sabir Ahmed Smael Khaman[1]
Treefa Farouq Ismail[2]
Department of Biology, College of Education, Salahaddin University-Erbil, Erbil, Kurdistan Region, Iraq
[1]sabir.Smael@su.edu.krd
[2] treefa.ismail@su.edu.krd

Abstract

Colorectal cancer (CRC) is one of the most frequent cancers worldwide and the leading cause of death annually. In recent years, the study of natural preventative agents and food components in addition to traditional treatments has seen an increase in interest and effort. Nowadays, novel procedures are constantly being researched, including nanotechnology-based cancer treatment, which is regarded as one of the most promising research directions for colon cancer. This experiment's goal was to determine if silver nanoparticles made from aqueous extracts of *Taraxacum officinale* leaves (TOL-AgNPs) could help prevent colon cancer in rats that had been given 1,2-dimethylhydrazine (DMH). Thirty-five rats have been allocated at random into five groups: control, DMH, TOL-AgNPs alone, TOL-AgNPs combined with DMH, and post-treated. DMH was administered intraperitoneally at a dosage of 30 mg/kg body weight once per week for eight weeks, while TOL-AgNPs were orally given at a dosage of 20 mg/kg body weight. UV-visible spectroscopy, FTIR spectrum, X-ray diffraction (XRD), SEM and EDAX, TEM examinations were utilized to characterize TOL-AgNPs. Hematological and biochemical tests were assessed additionally for markers of oxidative stress. Also, colon tissues were examined histopathologically. It was discovered that DMH elevated the hematological and biochemical parameters significantly ($P \leq 0.05$). TOL-AgNPs restored these measurements to an approximately normal range. According to a histopathological examination, the TOL-AgNPs exhibit anticancer effects in all nano-extract treatment groups. Our findings demonstrated that AgNPs produced utilizing the leaves of *T. officinale* have potent anticancer activity against DMH-induced colon cancer.

Keywords: Colon Cancer, Taraxacum officinale leaves, DMH, Green nanotechnology, Oxidative stress.

1. Introduction Colorectal cancer (CRC) is among the most prevalent kinds of gastrointestinal malignancies that have been widely researched globally. It ranks as the third most common reason for cancer-related death(Shelton, 2002). The etiology of CRC is characterized by the progressive and multi-step transformation of epithelial cells to a malignant phase via precancerous intermediates (Raju, 2008). already when colorectal polyps develop as precancerous lesions following colon carcinogenesis, aberrant crypt foci (ACF) are discovered as abnormal clumps in the colon and rectum lining(Kim et al., 2008). Diet has a big influence impact on the progression of colon cancer. In recent years, individuals often consumed natural compounds with significant medical potential. Enormous economic expansion and fast urbanization

[1] A part of the First Author's M. Sc. Thesis

pushed individuals to embrace a western food choices, which is high in fat, heavy in protein, lower in carbohydrates, and less in fiber. This imbalanced food is regarded as a significant key contributor to the rising prevalence of colon cancer. In order to minimize the incidence, the carcinoma of the colon, a diet full of fruits and vegetables has gained prominence since it involves numerous phytochemicals having unique pharmacological characteristics (Johnson and Mukhtar, 2007). Cancer chemotherapy's effectiveness is restricted by drug-induced side effects, multidrug resistance, and off-target binding. To determine the effectiveness of possible anti-cancer medications and to develop novel cancer treatments, it is important to produce cancer tumors in rats(Chidambaram et al., 2011).

Numerous carcinogens can cause tumors in rats' colons, but 1,2-Dimethylhydrazine (DMH) is the powerful procarcinogen that can cause tumors in rats' colons and rectums(Karthik Kumar et al., 2009, Sangeetha et al., 2010). DMH is thought to produce active intermediates in the liver, such as azoxymethane & methylazoxymethanol (MAM) that are then carried into the colon through the biliary(Fiala, 1977). Following DMH exposure, systemic circulation is shown to contain MAM, a long-lived metabolite. The frequency step in the metabolism of DMH is the enzymatic modification of MAM to an active aldehyde, which can be produced either spontaneously or by enzyme-catalyzed processes. This produces an alkylating methyldiazonium ion that can methylate cellular macromolecules(Wolter and Frank, 1982). Initiation, then promotion, and finally progression are the three stages of carcinogenesis, and each one depicts the genetic changes which motivate the gradual conversion of healthy cells to extremely cancerous descendants that could display continuously disrupted cellular and molecular signaling pathways(Sugimura, 1992, Hanahan and Weinberg, 2000).

There are numerous colon cancer treatments available, including surgeries, chemotherapy, and radiotherapy as a complementary therapy. However, due to ineffective anti-cancer drugs in targeted areas, these therapies are typically ineffective. As a result, alternate mechanisms for effective dose distribution should be discovered. Nanotechnology is a multidisciplinary area that encompasses numerous sciences, including engineering, physical, chemical, biological, and medical sciences. It is one of the most promising fields for treating cancer(Sengupta et al., 2005, Hamzehzadeh et al., 2016). In the field of medicine, nanomaterials have found usage in a variety of applications, including bioanalytical diagnostics and therapies, drug delivery systems, cancer therapy, and tissue-engineered scaffolds and tools. Metal nanoparticles can be created via a wide range of biological, chemical, physical & hybrid techniques. As a result, the toxic effects of the synthesis process are currently being eliminated by a green strategy known as green synthesis. The green synthesis process includes benefits including being non-toxic, inexpensive, environmentally friendly, and biocompatible. In this method, bacteria, fungi, algae, other microorganisms, and plants are utilized as caps and reductants from their extracellular and intracellular matrix(Klaine et al., 2012, Muralisankar et al., 2016). *Taraxacum officinale*, also called dandelion, is a blooming herbaceous perennial plant in the Asteraceae family. Despite its reputation as a weed, a dandelion leaf has a variety of pharmacologically actively substances including terpenoids, triterpenes, and flavonoids (isoquercitrin, apigenin, caffeic acid, & chlorogenic acid, luteolin)(Xue et al., 2017). Dandelion has long been utilized as a therapeutic non-toxic herb with choleretic, diuretic, and anti-inflammatory characteristics. Additionally, it has been claimed to cure obesity, cancer, and cardiovascular disorders while also having

antioxidant properties. It grows on home and public lawns, along roadway edges, and beside waterways in many different nations(Dermesonluoglu et al., 2016). This study demonstrated a sustainable method for synthesizing AgNPs utilizing *T. officinale* leaf extract. In order to characterize the synthesized TOL-AgNPs, various microscopic and spectroscopic methods were used. The effectiveness of the biosynthesized TOL-AgNPs against 1,2-dimethylhydrazine was tested in order to assess their anticancer potential. The antioxidant and anticancer properties of synthetic TOL-AgNPs were also evaluated(Hu and Kitts, 2003, González-Castejón et al., 2012).

2. Materials And Methods

This research work was performed between September 2021 and June 2022 in the animal house, advanced physiology laboratory of the Department of Biology, College of Education in Salahaddin University-Erbil. The hematological-biochemical analysis was carried out at Central Laboratory Iraq-Erbil and the private Nobel Med laboratory.

2.1 Collection of plant and leaf extract preparation

After gathering freshly *T. officinale* leaves (TOL), they were air dry in the shade for ten days. The leaves had been dried and then ground into a powder in a mortar before being sieved. The extract is obtained by thoroughly mixing 5 grams of leaf powder with 50 milliliters of distilled water, boiling the solution at 60 degrees Celsius for 15 minutes, allowing it to cool, and then filtering it using Whatman No. 1 filter paper. The filtered extract of TOL was obtained for the production of AgNPs(Ajitha et al., 2014).

2.2 Biosynthesis of AgNPs from T. officinale extract

First, the optimal values for the production of AgNPs, including pH, temperature, and AgNO3 concentrations, were established. 10 milliliters of TOL extract were put into 90 milliliters of an aqueous mixture containing 1 mM of silver nitrate (AgNO3). TOL-AgNPs are formed as a result of chemical reduction, as seen by changing the colors from mild yellow to deep reddish-brown. The samples were preserved in an airtight bottle away from sunlight after being incubated at room temperature for 48 hrs(Jain et al., 2009). By centrifugation, the result of TOL-AgNP at 15000 rpm for 15 minutes, they were cleaned. TOL-AgNPs that were still semisolid was air dried and gathered as powder. After going through several characterizations, the produced TOL-AgNPs were put to use in biological applications(Alsalhi et al., 2016).

2.3 The Characterization of Synthesized TOL-AgNPs

2.3.1 **Visible-UV spectroscopy**

An ultraviolet-visible spectrum investigation verified the formation of AgNPs. The absorbance spectrum was obtained utilizing UV-visible spectroscopy (Perkin Elmer Spectrophotometer) at a wavelength between 200 and 700 nm.

2.3.2 **FTIR measurement**

The functional groups of produced AgNPs were investigated utilizing an FT-IR instrument (Shimadzu Company, Kyoto, Japan) to identify distinctive bands spanning between 400 and 4000 cm^{-1} with an intention of 2 cm^{-1}.

2.3.3 **The Examination of X-ray diffraction (XRD)**

The X-ray diffraction spectrum (XRD) of the TOL-AgNP was recorded using an X-ray diffractometer (Rigaku, Japan). With a time constant of 2 sec, the patterns were captured using 2θ scans from 30° to 80° at 0.04°/minute.

2.3.4 **SEM, EDX, and TEM study of TOL-AgNPs**

The SEM (scanning electron microscope), specifically a Carl Zeiss AG-EVO 50 (Zeiss, Germany), was used to examine the morphological properties of the artificial TOL-AgNP. In order to get these pictures, a dropping coat of TOL-AgNP was performed on a carbon-coated grid. An SEM apparatus was used to conduct studies of energy-dispersed X-rays, EDX on the NOVA 2200e equipment, and elemental mapping. Studies employing the TEM (transmission electron microscope) were conducted using a Philips CM100 Analyses Transmission Electron Microscopy, manufactured by Phillips in the Netherland.

2.4 TOL-AgNPs administration

The aqueous of TOL-AgNPs was produced and analyzed by advanced confirmation technology and given orally at a dosage of 20 mg/kg b. wt. (1/20 of the Median Lethal Dosage, LD50(Shousha et al., 2019).

2.5 Experimental induction of colorectal cancer in rats

To produce colon cancer, rats given one intraperitoneal (i.p.) infusion of DMH (1,2-dimethylhydrazine) at a concentration of 30 mg/kg b.wt. Every week for 8 weeks. As a result, the induced rats were utilized to assess the efficiency of the generated TOL-AgNPs against colorectal malignancy.

2.6 Experimental design

Thirty-five mature male Wistar albino rats (weighing 180–230 g) have been kept in wire-mesh cages with flooring. The animals have been housed in conventional circumstances ((22±2 ºC, 45 ± 5% moisture, and 12 hrs light-dark cycles)(Dongre et al., 2008). Throughout the trial of the experiment, the rats received conventional rat feed and had unlimited approach to tap water ad libitum. The experimental animals were handled and looked at in conformity with the National Institutes of Health Guidelines for the Utilization and Care of Laboratory Animals(Coskun et al., 2004, Abo-Elsoud et al., 2022).

Rats have been split into five groups at random (n=7): control group rats received a standard meal and given tap water, TOL-AgNPs treated group: Rats given a regular meal and were given TOL-AgNPs orally by gavage at a concentration of 20 mg/kg body weight for 56 days, Colon cancer caused groups: Rats have been intraperitoneally infused with DMH at a dose of 30 mg/kg one per weeks for 8 consecutive weeks, TOL-AgNPs simult.+ DMH-treated group: Rats have been injected intraperitoneally with DMH and given TOL-AgNPs spontaneously orally at a dosage of 20 mg/kg b. wt. for 56 total days, the final group was the DMH+TOL-AgNPs post-treated group: Rats received intraperitoneal injections of DMH at a dosage of 30 mg/kg b. wt. for 8 weeks, accompanied by orally administered TOL-AgNPs at a dosage of 20 mg/kg b. wt. for an additional 56 days.

2.7 Collection of tissue and blood samples

After the experiment, the rats were decapitated, and blood specimens were obtained by withdrawing the blood via cardiac puncture with a sterile disposable

plastic syringe for biochemical and hematological assay. A total of around 2 milliliters of blood was taken in an EDTA-containing tube as an anticoagulant, and about 5 ml of blood was gathered in gel tubes, which were then allowed to remain at room temperature for 30 min. before being gently centrifuging at 3000 rpm for fifteen min. Colon tissues were also collected, removed surgically, and cleaned in normal saline. Before being put in 10% formal saline for histological analysis, all of the colon tissues were taken from autopsies and cut into pieces.

Haematological and biochemical examination

An automatic blood analysis tool (Coulter/Swelab) was used to measure HB (haemoglobin), RBC (red blood cell), HCT (hematocrit), MCV (mean corpuscular volume), MCH (mean corpuscular haemoglobin), MCHC (mean corpuscular haemoglobin concentration), RDW (red cell distribution width), MPV (mean platelet volume), PLT (platelet count), WBC (white blood cell) and differential white blood cell (lymphocytes, monocytes and granulocytes). All typical biochemical markers were estimated using serum blood samples. ALT (alanine transaminase), AST (aspartate aminotransferase), & ALP (alkaline phosphatase) tests for liver enzymes. The biomarkers concentration of serum were evaluated by utilizing a standard kit (Biolabo) in accordance with the manufacturer's recommendations.

Biomarkers of Oxidative Stress Analysis

These parameters were tested chemically by utilizing serum to evaluate MDA (malondialdehyde) as an indication of LPO (lipid peroxidation) by the response of TBA (thiobarbituric acid) based on the Ohkawa et al. procedure. Serum glutathione (GSH) was also chemically examined utilizing commercial kits supplied by Beijing Solarbio Science & Technology Co., Ltd. (Beijing, China) (Ellman, 1959).

Histopathologic Analysis and Tissue Sectioning

After the study, when the animals became slaughtered, specimens of colonic tissues from separate groups were autopsied and histopathologically examined(Banchroft et al., 1996). All samples were quickly dehydrated in successive dilutions of alcohol mixtures (70%, 95%, and 100%) after being stored in (10%) buffered formaldehyde for 24 hrs. Tissue pieces have been cleaned with xylene before being embedded in paraffin wax. The rotary microtome was utilized to make paraffin blocks for sectioning at 5 microns thick. Tissue slices were collected on microscopic slides and deparaffinized by xylene before staining by eosin and hematoxylin (H and E) after mounting with DPX for observation under a light microscope to establish the existence of the orientation program. Histopathological alterations were also graded(Dommels et al., 2007).

2.8 Statistically Analysis

Overall data were statistically assessed utilizing the GraphPad Prism (version 9) and the one-way analysis of variance test (one-way ANOVA, Friedman test), accompanied by the Normality and Lognormality Tests. The findings have been demonstrated as the mean score and standard deviation (M±SD). When the variation among the groups' "P" values has been smaller than 0.05, the difference has been deemed statistically substantial.

3. RESULTS

UV-Visible spectroscopy

At room temperature, adding TOL extract to the silver nitrate (AgNO3) mixture caused it to turn from a bright yellow coloured mixture to a deep brown colour. However, the colour did not go darker after 15 minutes, indicating that the reaction was finished at that time. Using UV-visible spectroscopy for detection of the formation of TOL- AgNP. The generated nanomaterial showed greater SPR (surface plasmon resonance) of about 433 nm which suggests the synthesis of TOL-AgNP. The observed spectrum data also validated the creation of TOL-AgNPs (Fig.1). The distinguishing property of TOL-AgNPs is UV-absorbance at 433, which has been linked to SPR (Surface, Plasmon Absorption) of Ag+ (Hamelian et al., 2020).

Fourier transform infrared (FTIR) spectrum

The existence the variety of functional groups in biomaterials essential for the reduction process of Ag+ & capping or stabilizing of silver nanoparticles was determined using FT-IR spectroscopy. To determine the functional categories, the acquired intensity areas have been compared to typical ranges. The existence of a reducing agent with nanoparticles is illustrated by the absorbance peak in the FT-IR spectra of TOL-extract at 3421, 1452, 1112, 1078, 875, 700, and 619 cm-1 (Fig.2). The spectra's lines at 3421 cm-1 correspond to O-H bending vibrations, which indicate the appearance of phenol & alcohol. Stretching of aromatic C=C rings is the cause of the peak of about 1421 cm 1. Strong absorbance bands at 1452 and 1078 cm1 are attributed to the existence of carbonyl group stretching (C = O) & C-OH bending, respectively, in the extraction. According to several studies, these functional groups have a crucial part in the stabilizing and capping of AgNP (36, 37). The C-N shifting of amines is what causes the peaks at 1112 cm-1. Alkyl halides' typical C-Br stretching may be responsible for the band at 619 cm-1 areas(Niraimathi et al., 2013, Prakash et al., 2013).

Analysis of X-ray diffraction (XRD)

Powder XRD have been utilized to demonstrate the crystalline nature of TOL-AgNPs, shown in Fig.3. At 2θ = 38.2°, 44.1°, 64.83°, and 77.24°, which corresponded to the (111), (200), (220), and (311) lines, consecutively. Bragg's reflections were seen.

SEM and EDAX studies

The SEM images created from TOL-AgNPs showed that the AgNPs' morphology had somewhat aggregated with one another. AgNPs have a particle size dispersion that ranges from 30 to 50 nm. In Figures 4a, and b, the SEM micrographs of the TOL-AgNPs are shown. The particles look like spherical pellets and are agglomerated. Figure 4c represents the EDAX spectrum of Ag-NPs, chemical analysis of TOL-AgNP confirmed both the formation & purity of the produced material silver (Ag) peak around 2 keV(Prakash et al., 2013).

TEM studies

The virtually spherical form and size of the TOL-AgNPs in the TEM picture with a scale of 50 nm were visible. Higher magnification reveals a monodisperse of AgNPs with some black-colored fringes, suggesting that the phytochemicals in TOL extract have capped the NPs. According to TEM pictures, the created AgNPs had a

spherical form, negligible aggregation, and a variety of sizes (Fig.5). The chemicals in the extract accumulated and adhered to those on the Ag-NP surfaces, causing this agglomeration(Biswal and Misra, 2020).

Although the current investigation was intended to demonstrate the efficacy of TOL-extracts combined with AgNP against DMH-caused colon disorders, this was discovered as DMH generated detrimental impacts on the haematological & biochemical parameters throughout the test period.

Haematological Analysis

As demonstrated in Table 1, DMH had a non-significant effect on haematological parameters relating to the red blood cell indices (RBC, HB, HCT, MCV, MCH, and MCHC). With the comparison to the control group, it generated a substantial ($P \leq 0.05$) increase in (MPV, RDW, PLT, and WBC) along with their differential counting values. Although treatment with TOL-AgNPs resulted in a substantial ($P \leq 0.05$) decline in all of the above parameters in the TOL-AgNPs treatment groups in comparison to the DMH-caused colorectal cancer groups, it returned such parameters to ordinary levels throughout the post-treatment groups.

Estimation of Biochemical Analyses

Table 2 shows that the reactivity of liver function tests (ALT, AST, and ALP) was elevated considerably ($P \leq 0.05$) in the serum of DMH-caused colon malignancy in compared to the control group. These chemical tests displayed a substantial ($P \leq 0.05$) reduction in TOL-AgNPs treated groups in comparison to the DMH-produced colorectal cancer groups.

Estimation of Oxidative stress biomarkers

Figure 6a shows that the frequency of MDA in the DMH-caused colon cancerous group has been substantially greater ($P \leq 0.05$) in comparison to the control group. TOL-AgNPs concurrently treated the group at a dosage 20 mg/kg b.wt) substantially ($P \leq 0.05$) reduced MDA levels in comparison to the DMH-produced cancer groups. *T. officinale* nano-extract post-treated at a dosage of 20 mg/kg b. wt. substantially ($P \leq 0.05$) reduced MDA rates in comparesion to the DMH-caused carcinoma group. GSH levels were considerably lower ($P \leq 0.05$) in the DMH-induced cancer group in contrast to the control group. When compared to the DMH-caused cancer group, the TOL-AgNPs concurrently treated group had a substantial rise in GSH levels. TOL-AgNPs post-treatment considerably ($P \leq 0.05$) elevated GSH levels in contrast to the DMH-induced cancer group as shown in figure 6b.

Histopathological Examination

The microscopic examination of diseased tissue is central to cancer diagnosis and therapy. The most prevalent kind of colon cancer is colorectal adenocarcinoma, which develops in structures with intestinal glandular components. The Histopathologic results of the colon tissue of the animals in the control group revealed usual colon architecture with normal glandular epithelium and a massive volume of goblet cells (Fig. 7 A, B). In the DMH-treatment groups, dysplastic crypts, desquamation of the mucosal lining epithelium's tips, and irregular glandular tissue that displays a few infiltrations of inflammatory cells in the lamina propria along with the development of crypt abscesses were seen (Fig. 7 C). Along with severe mucosal

dysplasia of glandular epithelium, there was regional mucosal destruction with severe infiltration of inflammatory cells in the submucosal layers, displaying large lymphocytic follicles that caused loss of mucosal architecture. The hyperplastic colon mucosa revealed a combination of goblet and absorbent cells (Fig. 7 D). The colonic tissue of the DMH-treated group showed high-level dysplasia from DMH due to significant inflammatory cell permeation in the lamina propria of the mucosa & submucosa (Fig. 7E, F). As a result, the DMH induced circumstances for the formation of tumors in the treated rats. However, the histological sections of the concurrently treated and post-treated groups with TOL-AgNPs at an oral dosage of 20 mg/kg revealed that TOL-AgNPs preserved the mucous area to destruction as well as a noticeable decline in penetration of the inflammatory cells and submucosal swelling. Normal numbers of goblet cells in the glandular epithelium have been seen, and also did not generate epithelium shedding in the colon tissues, although there was some moderate hyperplasia inside the epithelial tissue (Fig. 7 G, H, and I, J) respectively. Tissue sections from the TOL-AgNP-treated group alone showed a normal structure that was equivalent to the control groups (Fig 7 K, L).

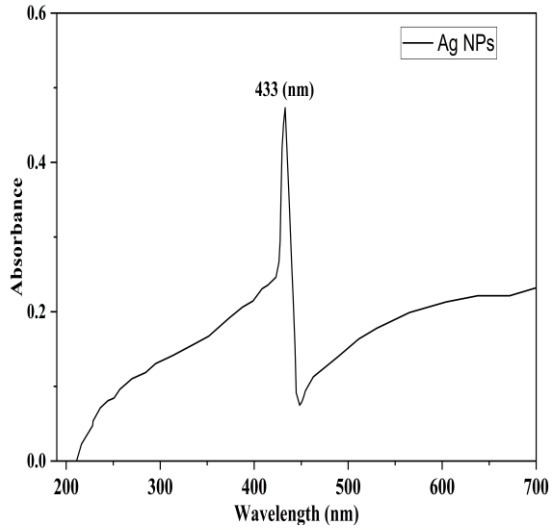

Figure 1. UV-visible spectrum of TOL-AgNPs

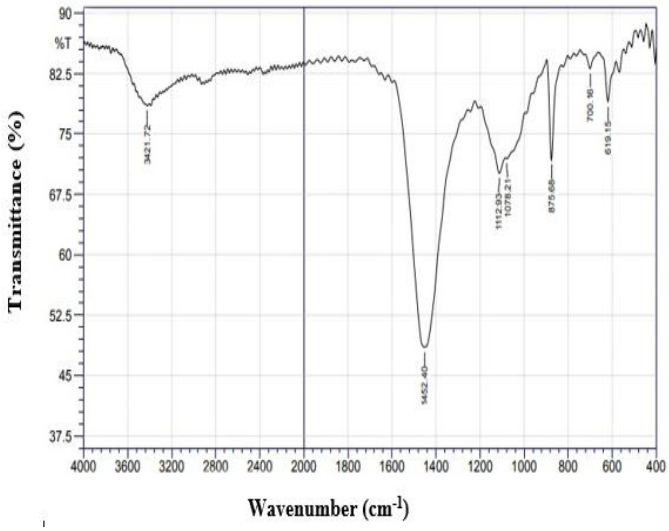

Figure 2. FTIR spectrum of TOL-AgNPs

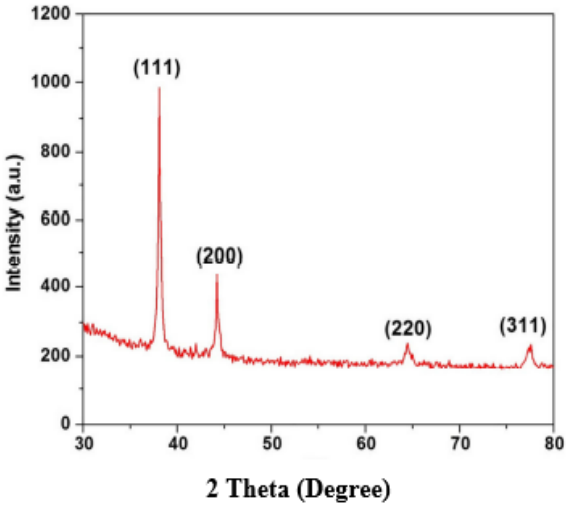

Figure 3. The XRD patterns of TOL-AgNP

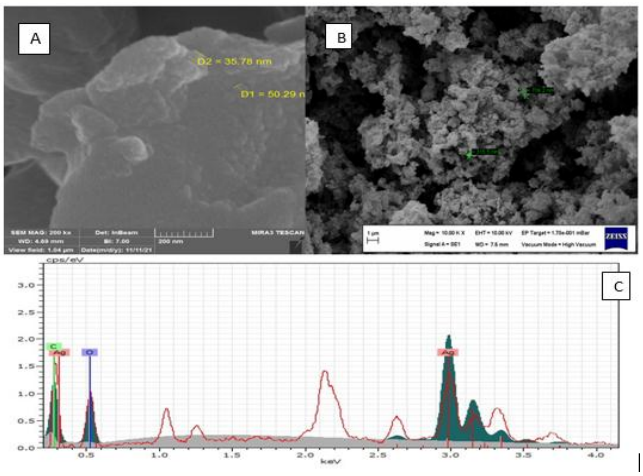

Figure 4. SEM and EDAX studies a, b: SEM images c: EDAX spectra of synthesis TOL- AgNPs

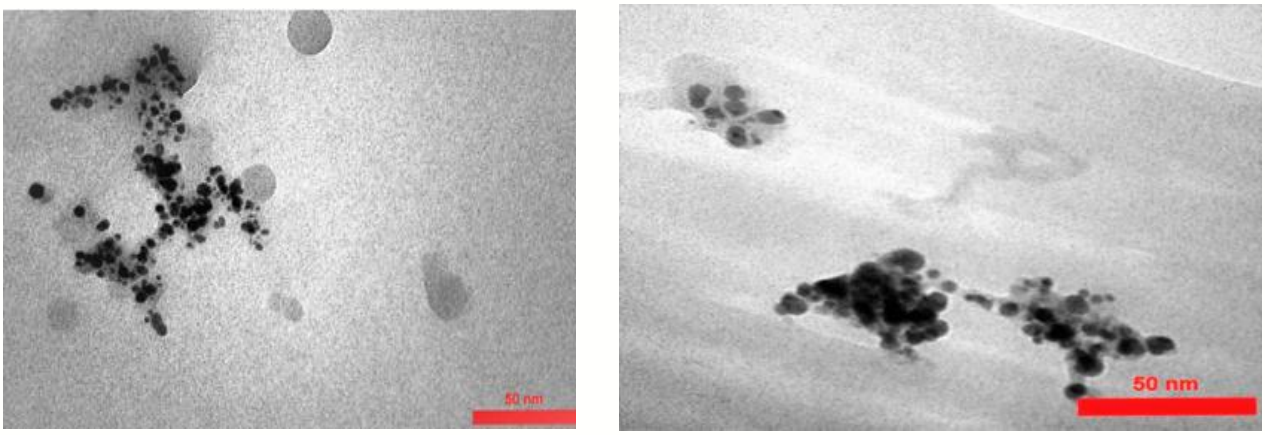

Figure 5. TEM picture of TOL-AgNP at a 50 nm resolutions

Table 1. The efficacy of *T. officinale* leaf extracts integrated Silver Nanoparticle AgNP versus DMH (1, 2-Dimethylhydrazine) Caused Colorectal Cancer on Different Haematological Parameters in Rats

Parameters	Experimental Groups				
	Control	Induced Cancer	*T.officinale* nano-extract Simult-treated	Post-treated	*T. officinale* nano-extract
Total RBC (10^{12}/L)	7.85±0.44b	6.2±0.46a	7.85±1.21a	7.47±0.28a	7.47±1.01b
Total WBC (x10^{9}/L)	8.81±0.61b	15.21±1.66a	10.17±1.78b	9.13±0.58b	8.9±2.14b
HB (g/dl)	12.48±1.27a	13.01±0.78a	12.76±3.68a	12.89±0.48 a	12.38±1.68 a
HCT %	42.28±2.71a	38.53±1.03a	42.02±1.52a	41.84±2.86 a	42.95±3.01 b
MCV (fl)	57.14±2.54a	55.17±2.98a	56.67±2.26a	56.14±6.53 a	58.07±1.06 a
MCH (pg)	16.97±0.91a	18.37±0.98a	16.6±0.76a	16.64±0.61 a	17.01±0.73 a
MCHC (g/dl)	36.31±1.45a	34.57±0.85a	35.01±0.85a	34.97±0.9a	35.54±0.59 a
GRAN %	20.47±1.91b	37.62±2.45a	23.2±1.82b	20.08±1.81 b	20.42±4.9b
LYM %	61.54±9.48b	77.21±3.61a	64.22±2.86b	61.75±3.48 b	61.55±5.47 b
RDW %	15.67±1.01b	21.12±0.89a	16.72±0.79b	15.75±0.88 b	15.65±0.94 b
MPV (fl)	6.28±0.71b	11.18±1.26a	7.22±1.03b	6.41±0.53b	6.31±0.7b
MONO %	10.36±3.02b	18.08±1.04a	10.97±1.61b	10.48±1.64 b	10.14±1.62 b
Platelets (10^{9}/L)	441.14±118. 64b	804.14±39.0 1a	510.85±118. 01b	460.57±66. 33b	443.42±49. 16b

The same letter in the column means a non-significant difference among parameters at P≤0.05.

Table 2. The efficacy of *T. officinale* Leaf Extracts integrated Silver Nanoparticle AgNP versus DMH (1, 2-Dimethylhydrazine) Caused Colorectal Cancer on Different Biochemical Parameters in Rats

Parameters	Experimental Groups			
	AST (U/L)	ALT (U/L)	ALP (U/L)	TSB (mg/dl)
Control	163.57±19.29b	48.42±3.45b	454.17±38.14b	0.06±0.02b
Induced Cancer	270.68±23.76a	96.94±25.09a	820.42±92.19a	0.36±0.19a
T.officinale nano-extract Simulate-treated	163.62±13.09b	48.97±5.23b	463.11±38.15b	0.07±0.07b
Post-treated	164.44±35.72b	48.41±4.52b	456.44±43.36b	0.08±0.07a
T. officinale nano-extract	162.05±10.17b	48.17±5.19b	448.62±26.97b	0.05±0.04b

The same letter in the column means a non-significant difference among parameters at P≤0.05.

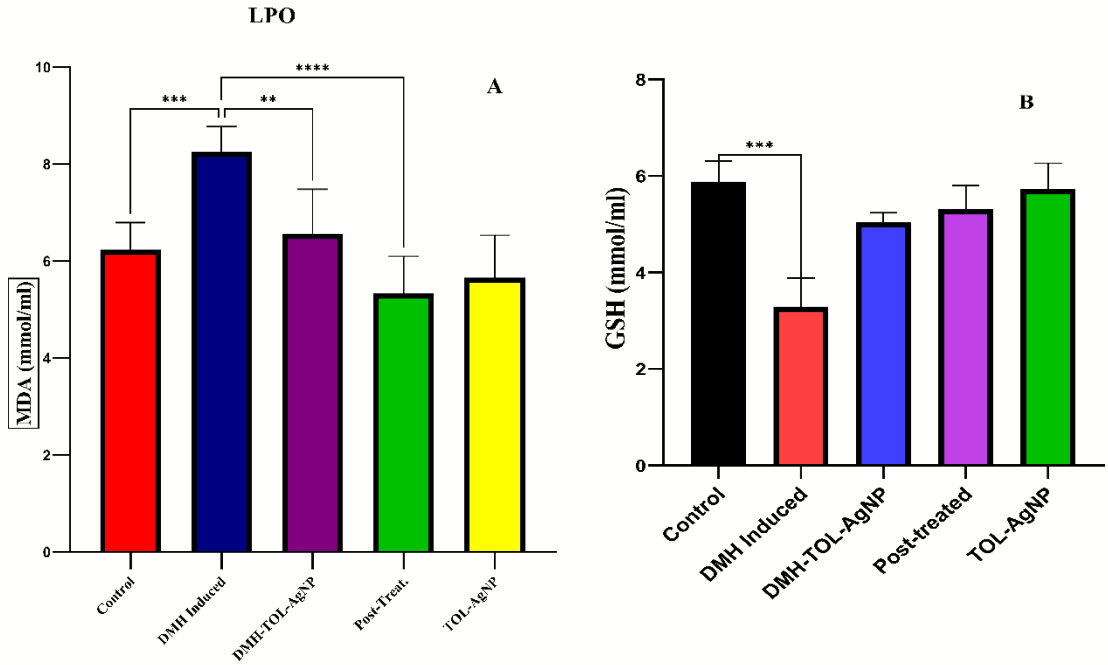

Figure 6. The efficacy of T. officinale Leaf Extracts integrated Silver Nanoparticles AgNP opposed to DMH (1, 2-Dimethylhydrazine) Caused Colorectal Cancer on the Biomarkers of Oxidative Stress in Rats

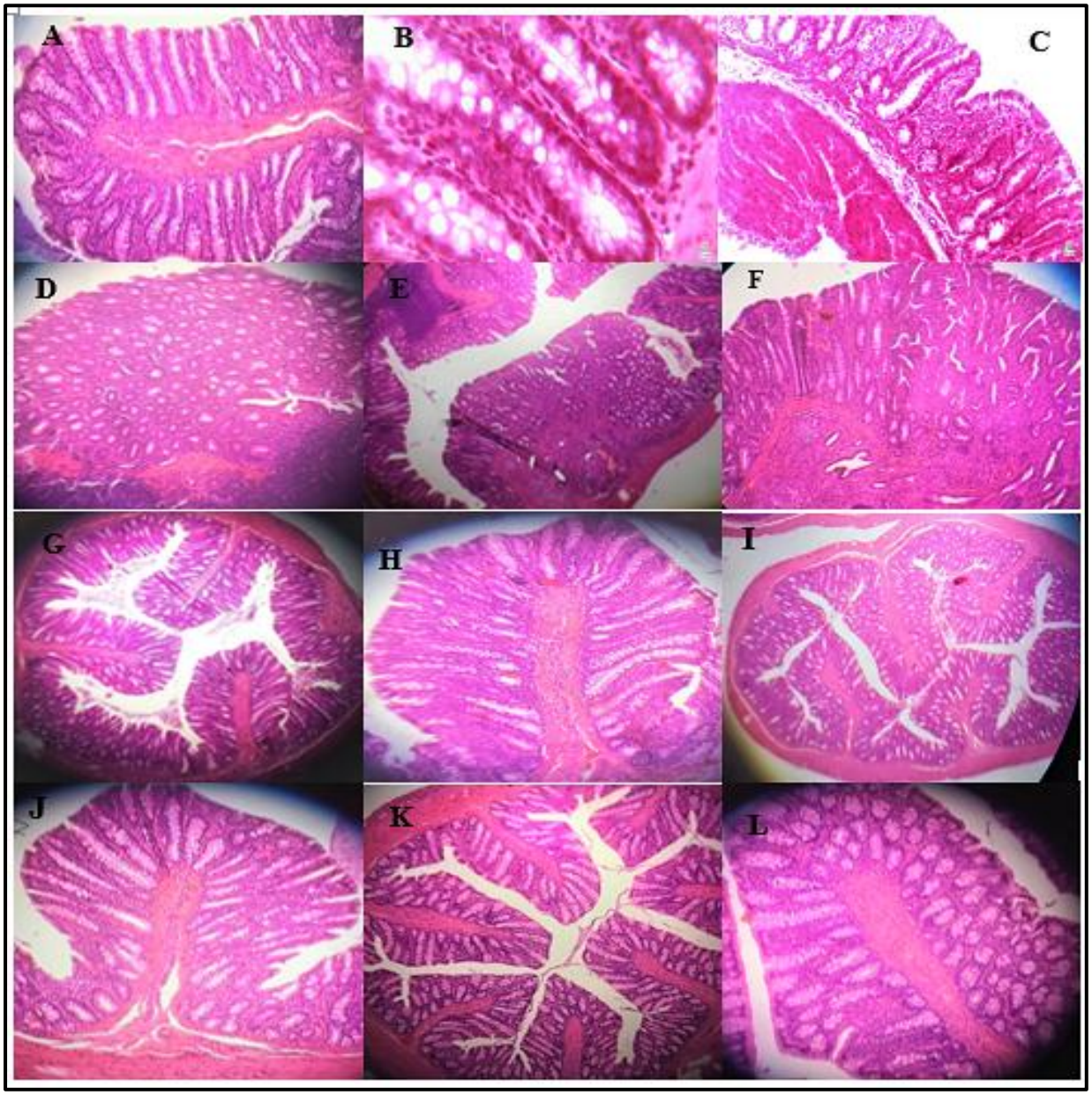

Figure 7. Histopathological analysis demonstrating the effectiveness of TOL-extracts against DMH-induced colorectal cancer on rat's colon tissues following addition of silver nanoparticles (AgNP). (A,B) The control group showed a clear number of goblet cells and a normal histological shape of the mucus with glandular shape (H&E, 10x, 40x, respectively); (C) the DMH-caused colon cancer group revealed dysplastic crypts with ulcerations of such tips with in previous sections and mucosal of epithelial layar (H &E, 20x); D) DMH-induced colon cancer group demonstrated high grade dysplasia developed clearly with huge infiltration of cell inflammation in lamina propria of the submucosa and mucus (H & E, 10x), E) The lamina propria of the submucosa and mucus in the DMH-induced colon cancer group clearly displayed high grade dysplasia development and large infiltration of inflammatory cells (H & E, 10x), F. magnification of criteria of malignancy of disorganization (H & E, 20x), G,H) DMH + TOL-AgNPs Simultaneously treated group showed approximately normal feature of colonic tissue with normal glandular mucosa, normal number of goblet cells, associated with some inflammatory cells

infiltration (H & E, 10x, 20x respectively), I,J) DMH Post-treated with TOL-AgNPs group showed colonic tissue near to normal as control tissue H&E (10x, 40x respectively), K,L) The group that received only TOL-AgNPs displayed normal histological architecture H&E (10x, x20 respectively).

4. DISCUSSION

An essential analytical tool for determining SPR and researching the optical characteristics of produced AgNPs is UV-visible absorbing spectroscopy. There was a colour change after adding TOL-extract to the AgNO3 solution, indicating that the Ag+ ions had been reduced to Ag0. many researchers said that the existence of higher polar phytoconstituents in the aqueous plant leaf extracts was what made nanoscales. Under ideal circumstances, the UV-vis measurements of the characteristic absorbance band at 433 nm proved that AgNPs were formed. In general, normal AgNPs exhibit typical SPR at wavelengths between 400 and 480 nm, which was also seen in the current study(Velmurugan et al., 2013, Nazeruddin et al., 2014, Saratale et al., 2017). Increased NP creation was the cause of the SPR peak's growth with incubation time(Ahmed et al., 2016, Saratale et al., 2018a). Particle size, morphology, internal particle distances, medium dielectric consistency, balancing particles, and surface-adsorbed components, on the other hand, all have a substantial influence on SPR patterns and AgNP characteristics. We performed UV-vis analytical research on our biosynthesized TOL-AgNPs. The peak at 433 nm stays the same, showing that biosynthesized TOL-AgNPs are good and making them more useful(Pal et al., 2007, Shankar et al., 2016).

The peak locations in the spectrum are used in FTIR spectroscopy to determine knowledge of the various operational groups. The TOL leaf extract was used in FTIR to determine potential biological molecules associated with the binding and elimination of AgNPs. The hydroxyl groups may form intermolecular hydrogen bonds, which would explain the peak's broadness(Majumdar et al., 2013). These peaks indicated that the *T. officinale* leaf extract contained phenolic and flavonoid acids. In the FTIR spectra of the fixed TOL-AgNPs, carbonyl units and aromatic circles were discovered to be implicated in nanoparticle production. The reduction of silver ions and the creation of matching AgNP may be caused by the existence of several pharmacologically potent bioactive chemicals in the leaf extracts, like a flavonoids and phenolic acids (chlorogenic acid and caffeic acid). According to certain research, in lacking of additional powerful binding reagents, these flavonoid and phenolic acids may interact with metal nanoparticle surfaces π-electrons and get deposited there. So, it seemed like the biomolecules in the leaf extracts had been reducing, binding, and fixing the AgNPs that were being made(Rostami-Vartooni et al., 2016, Saratale et al., 2018b).

The XRD patterns were utilized to evaluate the composition of the produced AgNPs and revealed 4 diffraction lines, 111, 200, 220, & 311, which were lines of Ag in accordance with the typical face-centered cubic structure of Ag. Additionally, the crystalline nature of the produced AgNP was verified by the high strength of the (111) reflection peak is compare to other reflections. The findings are steady with previous investigations, which showed comparable diffraction peaks of TOL-AgNPs(Ahmed et al., 2016, Saratale et al., 2017).

According to Rautela et al. SEM picture reveals morphological properties and size measurements of produced AgNPs(Rautela and Rani, 2019). Our findings demonstrated that the produced nanoparticles measured by SEM ranged in size from

35.78 to 50.29 nm. According to other investigations, AgNPs created utilizing *T. officinale* leaves extract were spherical in form and ranged in size between 30- 50 nm(Zhang et al., 2016). The biological molecules within rhizomes extraction that served as the capping layer of AgNP may be the cause of these size differences. Solvent evaporation during sample preparation caused NP accumulation. In several investigations, smaller, non-aggregated NPs decreased cytotoxically and increased penetration volume in certain diseases(Kumar et al., 2017, Devanesan et al., 2020). The TEM examination of TOL-AgNPs showed that they were uniformly smooth, well disseminated, and spherical in shape. It is possible to see the brilliant, black-colored cover, which suggests that natural compounds from TOL extracts may be important for the caps and stability of AgNP. Nevertheless, tiny agglomerates were seen, which may be because TOL-AgNPs' surface is covered with biological macromolecules(Mishra et al., 2014, Velmurugan et al., 2013).

Although the current work was intended to demonstrate the usefulness of TOL-extract combined with AgNP against DMH-caused colon cancer, these were discovered as DMH had diverse negative impacts at different haematological and biochemical values throughout the elicitation stages. Animal models must be used to examine the pathogenesis of colorectal cancers and to evaluate potential alternative therapies. Hematological measures could be utilized to evaluate an animal's adverse effects on blood components, as well as to explain the blood-related activities of chemical compounds or plant extracts(Ashafa et al., 2009, ASC and Costa-Casagrande, 2018). DMH is widely recognized as causing changes in the hematology condition of rats. Most of these changes were attributed to oxidative stress, which is linked to both haematological abnormalities and the development of cancer(Childress, 2012). During the present investigation, the values for HB and MCH in the DMH colon-induced groups have been slightly greater than the control group, when the values for RBCs count, HCT, MCV, and MCHC count were somewhat lower, but the variation seemed statistically meaningless ($p>0.05$) for all parameters. This was consistent with the findings of (Aboulthana et al., 2020), who found that DMH-induced cancer groups did not cause significant changes in haematological data related to red blood cell indices (RBC, HB, HCT, MCV, MCH, and MCHC) for all groups. Recent research showed that DMH-induced colon cancer dramatically increased RDW levels. This was consistent with the findings of (Förhécz et al., 2009) which showed that RDW levels are higher in aggressive carcinoma that is followed by a protracted inflammation phase. Furthermore, the RDW score has been linked to colon cancerous metastases as well as accurately predicts advanced cancer stages(Lee et al., 2014, Yang et al., 2018). The MPV value is regarded to be an early indicator of the proliferation of platelets, which was found to be a significant elevation in DMH-induced colon cancer groups in our studies, which was consistent with (Lee et al., 2014) who confirmed that MPV was found to be separately related to the appearance of colorectal cancer, as there was a strong relationship among MPV as well as the phase of tumour nodules metastases. In the DMH-induced colon cancer group, PLT levels increased considerably adding to WBC and their variable WBC counts (lymphocyte, monocyte, and granulocyte). This may be related to inflammatory responses that caused bone marrow to create PLT and leukocytes, particularly lymphocytes, since white blood cells travel to inflammatory sites furthermore are attracted by platelets(Laoui et al., 2011, Vieira-de-Abreu et al., 2012). Furthermore, neutrophils are regarded as the first defense line and are quickly attracted to inflammation sites in response to inflammation mediators generated at the site of

damage. Recent research has shown that DMH may cause liver damage and hepatotoxicity(Coussens and Werb, 2002, Megaraj et al., 2014). DMH was observed to produce an rise in the amounts of (AST, ALT, and ALP) which are the most commonly utilized indicators to measure liver functions. This is in agreement the results of of (Moharib et al., 2014) who reported that DMH induced liver injury as a consequence of strong corrosive electrophiles (alkyl free radicals and carbonium ions) which destruct liver tissues, producing inflammation and, therefore, loss of membrane permeability. In the early stages of liver damage, the cytoplasm's enzymes might spill through hepatocellular into the circulation because the membrane permeability is increased. TOL-AgNPs normalized these parameters in all treated phases (preservation & treatment). Those could be explained by the existence of a diverse variety of polyphenolics which were elevated by the incorporation of AgNP, as proposed by(Abdelhady and Badr, 2016) and protected by(Mahmoud Aboulthana et al., 2019) who discovered TOL-AgNPs hold excessive amounts of bioactive substances with antioxidant capacity in comparison to the leaf extracts. As a consequence, these compounds demonstrated a strong capacity to protect membrane permeability toward ROS produced by DMH injection.

We had already shown the significance of oxidative stress in DMH-caused colon injury(Khan and Sultana, 2011). DMH is indeed a procarcinogen that's also converted to methylene free radicals, which produces hydroxyl radicals or hydrogen peroxide in the presence of metal ions that might lead to the development of cancer phases and LPO. Lipid peroxidation (LPO), or MDA production, would be the essential also significant indicator of oxidative destruction and following DMH treatment, an increased amount of MDA product LPO was detected(Dudeja and Brasitus, 1990, Sengottuvelan et al., 2006). Consistent with earlier publications, our findings demonstrated a considerable rise in MDA levels after DMH therapy. TOL-AgNPs substantially reduce MDA levels in both the simultaneously treated and post-treated groups, and the findings are consistent with(Hamiza et al., 2012) where TOL-AgNPs have been demonstrated to be efficacious against colon damage. Free radicals are eliminated in biological systems by antioxidants (enzymatic and non-enzymatic), which serve as key defensive mechanisms versus free radicals(Ahmad and Sultana, 2012, Nandhakumar et al., 2012). GSH as well as its oxidizing analogue are important components of the cell's redox buffer system. GSH may operate as not an enzymatic scavenger through direct interaction with the SH groups of ROS or as a cofactor or coenzyme in the enzymatic detoxifying procedure for ROS. In our investigation, GSH values in rats administered by DMH decreased significantly, but those treated with TOL-AgNPs recovered typical GSH values, showing the protective effects of TOL-AgNPs. DMH therapy produces free radicals in colonic tissue, which GSH regulates by neutralizing the free radicals. As a result, DMH therapy reduces the levels of enzymatic antioxidants(Sengottuvelan et al., 2006). Both of the groups that were treated with TOL-AgNPs at the same time and the group that was treated afterward substantially restored these levels to normal(Rajeshkumar and Kuttan, 2003, Khan et al., 2012, Baskar et al., 2012).

To analyze the colorectal cancer progression in the DMH-induced groups as well as to test the therapeutic efficacy and anticancer potential of TOL-AgNPs against DMH-induced colon cancer,where the colon tissues of all the testing animals are histopathologically examined. The colon tissue's mucosal layer showed hyperplasia, dysplasia, and adenoma formation in the group exposed to carcinogens. The restoration of the colon tissue's natural cellular architecture is significantly reduced as

a result of the TOL-AgNPs therapy. After being treated with TOL-AgNPs, the hyperplastic lesion significantly decreased, and the goblet cells got back to their normal shape. These occurrences illustrate the efficacy of TOL-AgNPs in inhibiting colon cancer induced by DMH in rats. Previous research has shown the effectiveness of plant leaf AgNP efficacy versus many cellular diseases, such as rat spleen cells(Sengottaiyan et al., 2016) where malignant cells survival was markedly decreased in mice treated with AgNP(Jeyaprakash et al., 2020). In addition, the research by Murugesan et al. revealed, that human cervical cancer cell lines were more responsive to the toxic effectiveness of plant-based AgNPs. According to our findings, the synthetic TOL- AgNPs may have anti-oxidative and anti-tumour characteristics against DMH-caused colorectal cancer in rats(Murugesan et al., 2019).

5. CONCLUSION

In this study, green biosynthesized silver nanoparticles TOL-AgNPs were found to have an antiproliferative potential on rat colon cancer. One of the greatest methods of understanding the underlying structure of tumorigenesis and development, in addition to complete therapeutic options, is to use a rodent model for colorectal cancer. According to the current study, such antioxidants , anti-inflammation, and anti-tumour enhancing potent of TOL-AgNP against DMH-caused colon toxicity and neoplasia transformations through lowering amounts of the hematologic and biochemical parameters as well as restoring their amounts to standard levels across all nano-extract treatment groups. Additionally, the decrement in damages caused by DMH in animals treated was revealed by microscopic proofs that showed considerable anti-tumor activity.

References

ABDELHADY, N. M. & BADR, K. A. 2016. Comparative study of phenolic content, antioxidant potentials and cytotoxic activity of the crude and green synthesized silver nanoparticles′ extracts of two Phlomis species growing in Egypt. *Journal of Pharmacognosy and Phytochemistry,* 5**,** 377-383.

ABO-ELSOUD, R. A. E. A., AHMED MOHAMED ABDELAZIZ, S., ATTIA ABD ELDAIM, M. & HAZZAA, S. M. 2022. Moringa oleifera alcoholic extract protected stomach from bisphenol A–induced gastric ulcer in rats via its anti-oxidant and anti-inflammatory activities. *Environmental Science and Pollution Research***,** 1-12.

ABOULTHANA, W. M., IBRAHIM, N. E., OSMAN, N. M., SEIF, M. M., HASSAN, A. K., YOUSSEF, A. M., EL-FEKY, A. M. & MADBOLI, A. A. 2020. Evaluation of the Biological Efficiency of Silver Nanoparticles Biosynthesized Using Croton tiglium L. Seeds Extract against Azoxymethane Induced Colon Cancer in Rats. *Asian Pac J Cancer Prev,* 21**,** 1369-1389.

AHMAD, S. T. & SULTANA, S. 2012. Tannic acid mitigates cisplatin-induced nephrotoxicity in mice. *Hum Exp Toxicol,* 31**,** 145-56.

AHMED, S., AHMAD, M., SWAMI, B. L. & IKRAM, S. 2016. A review on plants extract mediated synthesis of silver nanoparticles for antimicrobial applications: A green expertise. *J Adv Res,* 7**,** 17-28.

AJITHA, B., REDDY, Y. A. & REDDY, P. S. 2014. Biogenic nano-scale silver particles by Tephrosia purpurea leaf extract and their inborn antimicrobial activity. *Spectrochim Acta A Mol Biomol Spectrosc,* 121**,** 164-72.

ALSALHI, M. S., DEVANESAN, S., ALFURAYDI, A. A., VISHNUBALAJI, R., MUNUSAMY, M. A., MURUGAN, K., NICOLETTI, M. & BENELLI, G. 2016. Green synthesis of silver nanoparticles using Pimpinella anisum seeds: antimicrobial activity and cytotoxicity on human neonatal skin stromal cells and colon cancer cells. *Int J Nanomedicine,* 11**,** 4439-4449.

ASC, D. E.-S. & COSTA-CASAGRANDE, T. A. 2018. ANIMAL MODELS FOR COLORECTAL CANCER. *Arq Bras Cir Dig,* 31**,** e1369.

ASHAFA, A., YAKUBU, M., GRIERSON, D. & AFOLAYAN, A. 2009. Toxicological evaluation of the aqueous extract of Felicia muricata Thunb. leaves in Wistar rats. *African Journal of Biotechnology,* 8.

BANCHROFT, J., STEVENS, A. & TURNER, D. 1996. Theory and practice of histological techniques. Churchil Livingstone, New York, London, San Francisco, Tokyo.

BASKAR, A. A., AL NUMAIR, K. S., GABRIEL PAULRAJ, M., ALSAIF, M. A., MUAMAR, M. A. & IGNACIMUTHU, S. 2012. β-sitosterol prevents lipid peroxidation and improves antioxidant status and histoarchitecture in rats with 1,2-dimethylhydrazine-induced colon cancer. *J Med Food,* 15**,** 335-43.

BISWAL, A. K. & MISRA, P. K. 2020. Biosynthesis and characterization of silver nanoparticles for prospective application in food packaging and biomedical fields. *Materials Chemistry and Physics,* 250**,** 123014.

CHIDAMBARAM, M., MANAVALAN, R. & KATHIRESAN, K. 2011. Nanotherapeutics to overcome conventional cancer chemotherapy limitations. *J Pharm Pharm Sci,* 14**,** 67-77.

CHILDRESS, M. O. 2012. Hematologic abnormalities in the small animal cancer patient. *Vet Clin North Am Small Anim Pract,* 42**,** 123-55.

COSKUN, O., OCAKCI, A., BAYRAKTAROGLU, T. & KANTER, M. 2004. Exercise training prevents and protects streptozotocin-induced oxidative stress and beta-cell damage in rat pancreas. *Tohoku J Exp Med,* 203**,** 145-54.

COUSSENS, L. M. & WERB, Z. 2002. Inflammation and cancer. *Nature,* 420**,** 860-7.

DERMESONLUOGLU, E., FILERI, K., ORFANOUDAKI, A., TSEVDOU, M., TSIRONI, T. & TAOUKIS, P. 2016. Modelling the microbial spoilage and quality decay of pre-packed dandelion leaves as a function of temperature. *Journal of Food Engineering,* 184**,** 21-30.

DEVANESAN, S., PONMURUGAN, K., ALSALHI, M. S. & AL-DHABI, N. A. 2020. Cytotoxic and Antimicrobial Efficacy of Silver Nanoparticles Synthesized Using a Traditional Phytoproduct, Asafoetida Gum. *Int J Nanomedicine,* 15**,** 4351-4362.

DOMMELS, Y. E., BUTTS, C. A., ZHU, S., DAVY, M., MARTELL, S., HEDDERLEY, D., BARNETT, M. P., MCNABB, W. C. & ROY, N. C. 2007. Characterization of intestinal inflammation and identification of related gene expression changes in mdr1a(-/-) mice. *Genes Nutr,* 2**,** 209-23.

DONGRE, S. H., BADAMI, S. & GODAVARTHI, A. 2008. Antitumor activity of Hypericum hookerianum against DLA induced tumor in mice and its possible mechanism of action. *Phytother Res,* 22**,** 23-9.

DUDEJA, P. K. & BRASITUS, T. A. 1990. 1,2-Dimethylhydrazine-induced alterations in lipid peroxidation in preneoplastic and neoplastic colonic tissues. *Biochim Biophys Acta,* 1046**,** 267-70.

ELLMAN, G. L. 1959. Tissue sulfhydryl groups. *Arch Biochem Biophys,* 82**,** 70-7.

FIALA, E. S. 1977. Investigations into the metabolism and mode of action of the colon carcinogens 1,2-dimethylhydrazine and azoxymethane. *Cancer,* 40**,** 2436-45.

FÖRHÉCZ, Z., GOMBOS, T., BORGULYA, G., POZSONYI, Z., PROHÁSZKA, Z. & JÁNOSKUTI, L. 2009. Red cell distribution width in heart failure: prediction of clinical events and relationship with markers of ineffective erythropoiesis, inflammation, renal function, and nutritional state. *Am Heart J,* 158**,** 659-66.

GONZÁLEZ-CASTEJÓN, M., VISIOLI, F. & RODRIGUEZ-CASADO, A. 2012. Diverse biological activities of dandelion. *Nutr Rev,* 70**,** 534-47.

HAMELIAN, M., ZANGENEH, M. M., SHAHMOHAMMADI, A., VARMIRA, K. & VEISI, H. 2020. Pistacia atlantica leaf extract mediated synthesis of silver nanoparticles and their antioxidant, cytotoxicity, and antibacterial effects under in vitro condition. *Applied Organometallic Chemistry,* 34**,** e5278.

HAMIZA, O. O., REHMAN, M. U., TAHIR, M., KHAN, R., KHAN, A. Q., LATEEF, A., ALI, F. & SULTANA, S. 2012. Amelioration of 1,2 Dimethylhydrazine (DMH) induced colon oxidative stress, inflammation and tumor promotion response by tannic acid in Wistar rats. *Asian Pac J Cancer Prev,* 13**,** 4393-402.

HAMZEHZADEH, L., IMANPARAST, A., TAJBAKHSH, A., REZAEE, M. & PASDAR, A. 2016. New approaches to use Nanoparticles for treatment of colorectal cancer; a brief review. *Nanomedicine Research Journal,* 1**,** 59-68.

HANAHAN, D. & WEINBERG, R. A. 2000. The hallmarks of cancer. *Cell,* 100**,** 57-70.

HU, C. & KITTS, D. D. 2003. Antioxidant, prooxidant, and cytotoxic activities of solvent-fractionated dandelion (Taraxacum officinale) flower extracts in vitro. *J Agric Food Chem,* 51**,** 301-10.

JAIN, D., DAIMA, H. K., KACHHWAHA, S. & KOTHARI, S. SL: Synthesis of plantmediated silver nanoparticles using papaya fruit extract and evaluation of their anti microbial activities. Digest Journal of Nanomaterials and Biostructures, 2009. Citeseer.

JEYAPRAKASH, K., ALSALHI, M. S. & DEVANESAN, S. 2020. Anticancer and antioxidant efficacy of silver nanoparticles synthesized from fruit of Morinda citrifolia Linn on Ehrlich ascites carcinoma mice. *Journal of King Saud University-Science,* 32**,** 3181-3186.

JOHNSON, J. J. & MUKHTAR, H. 2007. Curcumin for chemoprevention of colon cancer. *Cancer Lett,* 255**,** 170-81.

KARTHIK KUMAR, V., VENNILA, S. & NALINI, N. 2009. Modifying effects of morin on the development of aberrant crypt foci and bacterial enzymes in experimental colon cancer. *Food Chem Toxicol,* 47**,** 309-15.

KHAN, R., KHAN, A. Q., QAMAR, W., LATEEF, A., TAHIR, M., REHMAN, M. U., ALI, F. & SULTANA, S. 2012. Chrysin protects against cisplatin-induced colon. toxicity via amelioration of oxidative stress and apoptosis: probable role of p38MAPK and p53. *Toxicol Appl Pharmacol,* 258**,** 315-29.

KHAN, R. & SULTANA, S. 2011. Farnesol attenuates 1,2-dimethylhydrazine induced oxidative stress, inflammation and apoptotic responses in the colon of Wistar rats. *Chem Biol Interact,* 192**,** 193-200.

KIM, J., NG, J., AROZULLLAH, A., EWING, R., LLOR, X., CARROLL, R. E. & BENYA, R. V. 2008. Aberrant crypt focus size predicts distal polyp histopathology. *Cancer Epidemiol Biomarkers Prev*, 17**,** 1155-62.

KLAINE, S. J., KOELMANS, A. A., HORNE, N., CARLEY, S., HANDY, R. D., KAPUSTKA, L., NOWACK, B. & VON DER KAMMER, F. 2012. Paradigms to assess the environmental impact of manufactured nanomaterials. *Environ Toxicol Chem*, 31**,** 3-14.

KUMAR, B., SMITA, K., CUMBAL, L. & DEBUT, A. 2017. Green synthesis of silver nanoparticles using Andean blackberry fruit extract. *Saudi J Biol Sci*, 24**,** 45-50.

LAOUI, D., VAN OVERMEIRE, E., MOVAHEDI, K., VAN DEN BOSSCHE, J., SCHOUPPE, E., MOMMER, C., NIKOLAOU, A., MORIAS, Y., DE BAETSELIER, P. & VAN GINDERACHTER, J. A. 2011. Mononuclear phagocyte heterogeneity in cancer: different subsets and activation states reaching out at the tumor site. *Immunobiology*, 216**,** 1192-202.

LEE, H., KONG, S. Y., SOHN, J. Y., SHIM, H., YOUN, H. S., LEE, S., KIM, H. J. & EOM, H. S. 2014. Elevated red blood cell distribution width as a simple prognostic factor in patients with symptomatic multiple myeloma. *Biomed Res Int*, 2014**,** 145619.

MAHMOUD ABOULTHANA, W., YOUSSEF, A., M EL-FEKY, A., EL-SAYED IBRAHIM, N., M SEIF, M. & KAMAL HASSAN, A. 2019. Evaluation of antioxidant efficiency of Croton tiglium L. seeds extracts after incorporating silver nanoparticles. *Egyptian Journal of Chemistry*, 62**,** 181-200.

MAJUMDAR, R., BAG, B. G. & MAITY, N. 2013. Acacia nilotica (Babool) leaf extract mediated size-controlled rapid synthesis of gold nanoparticles and study of its catalytic activity. *International Nano Letters*, 3**,** 1-6.

MEGARAJ, V., DING, X., FANG, C., KOVALCHUK, N., ZHU, Y. & ZHANG, Q. Y. 2014. Role of hepatic and intestinal p450 enzymes in the metabolic activation of the colon carcinogen azoxymethane in mice. *Chem Res Toxicol*, 27**,** 656-62.

MISHRA, S., SINGH, B. R., SINGH, A., KESWANI, C., NAQVI, A. H. & SINGH, H. B. 2014. Biofabricated silver nanoparticles act as a strong fungicide against Bipolaris sorokiniana causing spot blotch disease in wheat. *PLoS One*, 9**,** e97881.

MOHARIB, S. A., ABD EL MAKSOUD, N., RAGAB, H. M. & SHEHATA, M. 2014. Anticancer activities of mushroom polysaccharides on chemically-induced colorectal cancer in rats. *Journal of Applied Pharmaceutical Science*, 4**,** 054-063.

MURALISANKAR, T., SARAVANA BHAVAN, P., RADHAKRISHNAN, S., SEENIVASAN, C. & SRINIVASAN, V. 2016. The effect of copper nanoparticles supplementation on freshwater prawn Macrobrachium rosenbergii post larvae. *J Trace Elem Med Biol*, 34**,** 39-49.

MURUGESAN, K., KOROTH, J., SRINIVASAN, P. P., SINGH, A., MUKUNDAN, S., KARKI, S. S., CHOUDHARY, B. & GUPTA, C. M. 2019. Effects of green synthesised silver nanoparticles (ST06-AgNPs) using curcumin derivative (ST06) on human cervical cancer cells (HeLa) in vitro and EAC tumor bearing mice models. *Int J Nanomedicine*, 14**,** 5257-5270.

NANDHAKUMAR, R., SALINI, K. & NIRANJALI DEVARAJ, S. 2012. Morin augments anticarcinogenic and antiproliferative efficacy against 7,12-

dimethylbenz(a)-anthracene induced experimental mammary carcinogenesis. *Mol Cell Biochem,* 364**,** 79-92.

NAZERUDDIN, G., PRASAD, N., PRASAD, S., SHAIKH, Y., WAGHMARE, S. & ADHYAPAK, P. 2014. Coriandrum sativum seed extract assisted in situ green synthesis of silver nanoparticle and its anti-microbial activity. *Industrial Crops and Products,* 60**,** 212-216.

NIRAIMATHI, K. L., SUDHA, V., LAVANYA, R. & BRINDHA, P. 2013. Biosynthesis of silver nanoparticles using Alternanthera sessilis (Linn.) extract and their antimicrobial, antioxidant activities. *Colloids Surf B Biointerfaces,* 102**,** 288-91.

PAL, S., TAK, Y. K. & SONG, J. M. 2007. Does the antibacterial activity of silver nanoparticles depend on the shape of the nanoparticle? A study of the Gram-negative bacterium Escherichia coli. *Appl Environ Microbiol,* 73**,** 1712-20.

PRAKASH, P., GNANAPRAKASAM, P., EMMANUEL, R., AROKIYARAJ, S. & SARAVANAN, M. 2013. Green synthesis of silver nanoparticles from leaf extract of Mimusops elengi, Linn. for enhanced antibacterial activity against multi drug resistant clinical isolates. *Colloids Surf B Biointerfaces,* 108**,** 255-9.

RAJESHKUMAR, N. V. & KUTTAN, R. 2003. Modulation of carcinogenic response and antioxidant enzymes of rats administered with 1,2-dimethylhydrazine by Picroliv. *Cancer Lett,* 191**,** 137-43.

RAJU, J. 2008. Azoxymethane-induced rat aberrant crypt foci: relevance in studying chemoprevention of colon cancer. *World J Gastroenterol,* 14**,** 6632-5.

RAUTELA, A. & RANI, J. 2019. Green synthesis of silver nanoparticles from Tectona grandis seeds extract: characterization and mechanism of antimicrobial action on different microorganisms. *Journal of Analytical Science and Technology,* 10**,** 1-10.

ROSTAMI-VARTOONI, A., NASROLLAHZADEH, M. & ALIZADEH, M. 2016. Green synthesis of seashell supported silver nanoparticles using Bunium persicum seeds extract: Application of the particles for catalytic reduction of organic dyes. *J Colloid Interface Sci,* 470**,** 268-275.

SANGEETHA, N., ARANGANATHAN, S., PANNEERSELVAM, J., SHANTHI, P., RAMA, G. & NALINI, N. 2010. Oral supplementation of silibinin prevents colon carcinogenesis in a long term preclinical model. *Eur J Pharmacol,* 643**,** 93-100.

SARATALE, G. D., SARATALE, R. G., BENELLI, G., KUMAR, G., PUGAZHENDHI, A., KIM, D.-S. & SHIN, H.-S. 2017. Anti-diabetic potential of silver nanoparticles synthesized with Argyreia nervosa leaf extract high synergistic antibacterial activity with standard antibiotics against foodborne bacteria. *Journal of Cluster Science,* 28**,** 1709-1727.

SARATALE, R. G., SHIN, H. S., KUMAR, G., BENELLI, G., GHODAKE, G. S., JIANG, Y. Y., KIM, D. S. & SARATALE, G. D. 2018a. Exploiting fruit byproducts for eco-friendly nanosynthesis: Citrus × clementina peel extract mediated fabrication of silver nanoparticles with high efficacy against microbial pathogens and rat glial tumor C6 cells. *Environ Sci Pollut Res Int,* 25**,** 10250-10263.

SARATALE, R. G., SHIN, H. S., KUMAR, G., BENELLI, G., KIM, D. S. & SARATALE, G. D. 2018b. Exploiting antidiabetic activity of silver nanoparticles synthesized using Punica granatum leaves and anticancer

potential against human liver cancer cells (HepG2). *Artif Cells Nanomed Biotechnol,* 46**,** 211-222.

SENGOTTAIYAN, A., MYTHILI, R., SELVANKUMAR, T., ARAVINTHAN, A., KAMALA-KANNAN, S., MANOHARAN, K., THIYAGARAJAN, P., GOVARTHANAN, M. & KIM, J.-H. 2016. Green synthesis of silver nanoparticles using Solanum indicum L. and their antibacterial, splenocyte cytotoxic potentials. *Research on Chemical Intermediates,* 42**,** 3095-3103.

SENGOTTUVELAN, M., SENTHILKUMAR, R. & NALINI, N. 2006. Modulatory influence of dietary resveratrol during different phases of 1,2-dimethylhydrazine induced mucosal lipid-peroxidation, antioxidant status and aberrant crypt foci development in rat colon carcinogenesis. *Biochim Biophys Acta,* 1760**,** 1175-83.

SENGUPTA, S., EAVARONE, D., CAPILA, I., ZHAO, G., WATSON, N., KIZILTEPE, T. & SASISEKHARAN, R. 2005. Temporal targeting of tumour cells and neovasculature with a nanoscale delivery system. *Nature,* 436**,** 568-72.

SHANKAR, P. D., SHOBANA, S., KARUPPUSAMY, I., PUGAZHENDHI, A., RAMKUMAR, V. S., ARVINDNARAYAN, S. & KUMAR, G. 2016. A review on the biosynthesis of metallic nanoparticles (gold and silver) using bio-components of microalgae: Formation mechanism and applications. *Enzyme Microb Technol,* 95**,** 28-44.

SHELTON, B. K. 2002. Introduction to colorectal cancer. *Semin Oncol Nurs,* 18**,** 2-12.

SHOUSHA, W. G., ABOULTHANA, W. M., SALAMA, A. H., SALEH, M. H. & ESSAWY, E. A. 2019. Evaluation of the biological activity of Moringa oleifera leaves extract after incorporating silver nanoparticles, in vitro study. *Bulletin of the National Research Centre,* 43**,** 1-13.

SUGIMURA, T. 1992. Multistep carcinogenesis: a 1992 perspective. *Science,* 258**,** 603-7.

VELMURUGAN, P., LEE, S. M., IYDROOSE, M., LEE, K. J. & OH, B. T. 2013. Pine cone-mediated green synthesis of silver nanoparticles and their antibacterial activity against agricultural pathogens. *Appl Microbiol Biotechnol,* 97**,** 361-8.

VIEIRA-DE-ABREU, A., CAMPBELL, R. A., WEYRICH, A. S. & ZIMMERMAN, G. A. 2012. Platelets: versatile effector cells in hemostasis, inflammation, and the immune continuum. *Semin Immunopathol,* 34**,** 5-30.

WOLTER, S. & FRANK, N. 1982. Metabolism of 1,2-dimethylhydrazine in isolated perfused rat liver. *Chem Biol Interact,* 42**,** 335-44.

XUE, Y., ZHANG, S., DU, M. & ZHU, M.-J. 2017. Dandelion extract suppresses reactive oxidative species and inflammasome in intestinal epithelial cells. *Journal of Functional Foods,* 29**,** 10-18.

YANG, D., QUAN, W., WU, J., JI, X., DAI, Y., XIAO, W., CHEW, H., SUN, Z. & LI, D. 2018. The value of red blood cell distribution width in diagnosis of patients with colorectal cancer. *Clin Chim Acta,* 479**,** 98-102.

ZHANG, X. F., LIU, Z. G., SHEN, W. & GURUNATHAN, S. 2016. Silver Nanoparticles: Synthesis, Characterization, Properties, Applications, and Therapeutic Approaches. *Int J Mol Sci,* 17.